Deglacial Ice Sheet Instabilities Induced by Proglacial Lakes

Aurélien Quiquet, Christophe Dumas, Didier Paillard, Gilles Ramstein, Catherine Ritz, Didier M. Roche

▶ **To cite this version:**

Aurélien Quiquet, Christophe Dumas, Didier Paillard, Gilles Ramstein, Catherine Ritz, et al.. Deglacial Ice Sheet Instabilities Induced by Proglacial Lakes. Geophysical Research Letters, 2021, 48 (9), pp.e2020GL092141. 10.1029/2020GL092141 . hal-03228350

HAL Id: hal-03228350
https://hal.science/hal-03228350

Submitted on 14 Jun 2021

HAL is a multi-disciplinary open access archive for the deposit and dissemination of scientific research documents, whether they are published or not. The documents may come from teaching and research institutions in France or abroad, or from public or private research centers.

L'archive ouverte pluridisciplinaire **HAL**, est destinée au dépôt et à la diffusion de documents scientifiques de niveau recherche, publiés ou non, émanant des établissements d'enseignement et de recherche français ou étrangers, des laboratoires publics ou privés.

Check for updates

AGU ADVANCING EARTH AND SPACE SCIENCE

Geophysical Research Letters

RESEARCH LETTER
10.1029/2020GL092141

Key Points:

- The North American proglacial lakes induce an ice sheet instability during the last deglaciation.
- This instability is mechanically driven even though it is triggered by surface mass balance.
- The instability could explain half of the mass loss when the ice sheet reaches the region of the present-day Hudson Bay.

Supporting Information:

Supporting Information may be found in the online version of this article.

Correspondence to:

A. Quiquet,
aurelien.quiquet@lsce.ipsl.fr

Citation:

Quiquet, A., Dumas, C., Paillard, D., Ramstein, G., Ritz, C., & Roche, D. M. (2021). Deglacial ice sheet instabilities induced by proglacial lakes. *Geophysical Research Letters*, *48*, e2020GL092141. https://doi.org/10.1029/2020GL092141

Received 20 DEC 2020
Accepted 14 APR 2021

© 2021. American Geophysical Union. All Rights Reserved.

Deglacial Ice Sheet Instabilities Induced by Proglacial Lakes

Aurélien Quiquet[1,2], Christophe Dumas[1], Didier Paillard[1], Gilles Ramstein[1], Catherine Ritz[3], and Didier M. Roche[1,4]

[1]Laboratoire des Sciences du Climat et de l'Environnement, LSCE/IPSL, CEA-CNRS-UVSQ, Université Paris-Saclay, Gif-sur-Yvette, France, [2]Now at NumClimSolutions, Palaiseau, France, [3]Université Grenoble Alpes, CNRS, IRD, Grenoble INP, IGE, Grenoble, France, [4]Faculty of Science, Cluster Earth and Climate, Vrije Universiteit Amsterdam, Amsterdam, The Netherlands

Abstract During the last deglaciation (21–7 kaBP), the gradual retreat of Northern Hemisphere ice sheet margins produced large proglacial lakes. While the climatic impacts of these lakes have been widely acknowledged, their role on ice sheet grounding line dynamics has received very little attention so far. Here, we show that proglacial lakes had dramatic implications for the North American ice sheet dynamics through a self-sustained mechanical instability which has similarities with the known marine ice sheet instability consequently providing fast retreat of large portions of the ice sheet over the continent. This instability mechanism is likely important in contributing to deglaciation of terrestrial glaciers and ice sheets with proglacial lakes at their margins as it can substantially accelerate the mass loss. Echoing our knowledge of Antarctic ice sheet dynamics, proglacial lakes are another manifestation of the importance of grounding line dynamics for ice sheet evolution.

Plain Language Summary The last deglaciation provides a unique opportunity to understand the mechanisms behind large-scale ice sheet collapses. However, the mass loss accelerations that occurred during the deglaciation remain only partially explained despite recent improvements of ice sheet models which now better represent ice dynamics than they used to. Here we use such a model to quantify for the first time the importance of proglacial lakes on the dynamics of the North American ice sheet during the last deglaciation. We show that these lakes could be responsible for large-scale ice sheet collapses due to a floatation instability. The proglacial lake ice sheet instability could be an additional mechanism explaining the rapid ice sheet retreat during the deglaciation.

1. Introduction

Proglacial lakes have formed, evolved and drained in response to ice sheet changes throughout the Pleistocene (Teller, 1995). These lakes form at an ice margin dammed by ice, bedrock and/or moraine in depressed basins. During the last deglaciation (21–7 kaBP), these lakes were a common feature of the Northern Hemisphere landscape, spanning a range of sizes reaching up several thousands of square kilometres in extent (Carrivick & Tweed, 2013). These lakes can be short-lived or last for several thousand years and may experience abrupt changes in water level (Teller & Leverington, 2004). These abrupt water level variations have sometimes resulted in large lake outbursts that probably had important consequences on the global climate owing to the large resulting freshwater flux to the oceans (Teller & Leverington, 2004). It is widely acknowledged, for example, that the abrupt drainage of Lake Agassiz-Ojibway at 8.2 kaBP, the largest known glacial lake on Earth, which existed for thousands of years, induced a widespread cooling of the Northern Hemisphere via a slowdown of the Atlantic circulation (Barber et al., 1999; Wiersma & Renssen, 2006). Proglacial lakes have also had an impact at the regional scale, in particular for ice sheet surface mass balance, reducing summer ablation and favoring ice growth (Hostetler et al., 2000; Krinner et al., 2004). As the climatic importance of these lakes is well established, it is surprising perhaps that their role in ice sheet mechanics has received very little attention so far, although their importance at the glacier scale has been demonstrated (Carrivick et al., 2020; Sutherland et al., 2020). Using conceptual models for ice ages, some authors have hypothesized that these lakes could be responsible for Pleistocene ice volume oscillations, favoring calving and thus enhancing rapid ice retreat (Fowler et al., 2013; Pollard, 1982). This hypothesis has hitherto been tested with comprehensive physically based numerical ice sheet models.

Sea-level archives suggest that the deglacial rate of sea level rise has been far from linear, with episodic rapid accelerations (Lambeck et al., 2014). These accelerations, referred to as melt-water pulses (MWPs; Abdul et al., 2016; Deschamps et al., 2012), suggest large-scale ice sheet collapses. So far, our understanding of the underlying processes leading to such events is limited. Several mechanisms could explain these large scale ice sheet collapses: (i) ice stream surges due to internal thermo-mechanical oscillations (Calov et al., 2002; MacAyeal, 1993); (ii) grounding line migration for marine ice sheets (DeConto & Pollard, 2016); or iii) strongly negative surface mass balance due to the surface elevation feedbacks (Abe-Ouchi et al., 2013; Gregoire et al., 2012). To date, only this last process has been used in modeling studies to successfully reproduce the largest deglacial abrupt sea level rise, the MWP-1A (14.65–14.31 kaBP), with a so-called saddle collapse mechanism (Gregoire et al., 2012, 2016) affecting the North American ice sheet (NAIS).

If less attention has been put on mechanical instabilities this is because although a fair amount of ice sheet simulations of Northern Hemisphere deglaciation are available in the literature, they were performed with a former generation of ice sheet models (Abe-Ouchi et al., 2013; Charbit et al., 2005; Heinemann et al., 2014; Ganopolski & Brovkin, 2017; Gregoire et al., 2012). In recent years, considerable improvements of the numerical representation of the grounding line dynamics in ice sheet models have been made. They now either use a very high spatial resolution at the ice margin to explicitly solve grounding line dynamics (Larour et al., 2012), in some cases with some sub-grid parametrisations (Winkelmann et al., 2011), or they impose an ice flux crossing the grounding line using analytically derived formulations (Schoof, 2007; Tsai et al., 2015). These newer models have a grounding line migration that is much more sensitive to changes in boundary conditions (mass balance and sea level (Pattyn et al., 2013)) with respect to the previous generation, in particular because they explicitly represent the marine ice sheet instability (MISI, Schoof, 2007; Weertman, 1974). The MISI lies in the fact that a grounding line located on a retrograde bed slope can only present an unstable equilibrium for which any initial retreat of the grounding line induces a further retreat until the proximal prograde slope. Only the lateral drag and the buttressing force exerted by the ice shelves can favor stability. Large portion of the present-day Antarctic ice sheet presents a grounding line in this configuration and basin-scale instabilities could have been already triggered (Favier et al., 2014).

During glacial periods, glacioisostatic depression produced overdeepened basins below the NAIS in which the proglacial lakes formed. The southern margin of the ice sheet was thus configured in a setting where MISI could likely have occurred, with a reverse gradient bedrock below sea level sloping toward the ice sheet interior. It is thus possible that grounding line instabilities could have occurred during the deglaciation at the continental margin of the NAIS. While the impact of proglacial lakes for glacier dynamics have been acknowledged (Carrivick et al., 2020; Sutherland et al., 2020), it is surprising that their role during the deglaciation of the NAIS has not been quantified with comprehensive models so far. In this study, we use a set of numerical experiments with an ice sheet model able to produce grounding line instabilities to study the impact of large proglacial lakes on ice sheet dynamics and to quantify their potential contribution to sea level rise accelerations during the last deglaciation.

2. Methods

In this work, we use the GRISLI ice sheet model (Quiquet, Dumas, et al., 2018) to simulate the evolution of the Northern Hemisphere ice sheets for the last 26 kyrs. We showed previously that the model was able to correctly reproduce the grounding line migration for the Antarctic ice sheet across the last four glacial-interglacial cycles (Quiquet, Dumas, et al., 2018). The model has been included in international intercomparison exercises for shorter time scales for both the Greenland and the Antarctic ice sheets (Goelzer et al., 2020; Levermann et al., 2020; Quiquet & Dumas, 2021a, 2021b; Seroussi et al., 2020; Sun et al., 2020) in which the model exhibits a response to changes in the forcings comparable to the other participating models. The ice flux at the sub-grid position of the grounding line (Tsai et al., 2015) is extrapolated to the nearest velocity grid points (Quiquet, Dumas, et al., 2018). Calving is based on a simple cut-off thickness threshold of 250 m below which ice is calved, since most present-day ice shelves have a thickness greater than this value. The model accounts for glacial isostasy with an elastic lithosphere - relaxed asthenosphere model. In the reference model set-up, any topographic depression below the contemporaneous eustatic sea level is assumed to be flooded with a water surface elevation at the eustatic sea level value. For model calibration, we perform an ensemble of 300 members, sampled with a latin hypercube methodology as in Quiquet, Dumas,

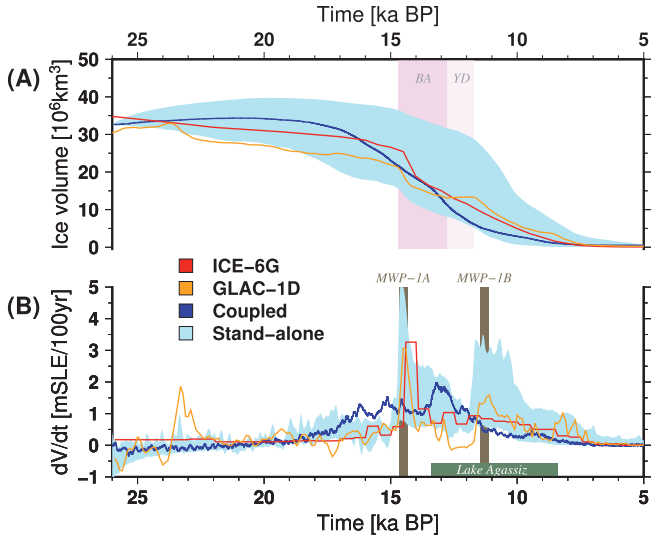

Figure 1. Temporal evolution. Simulated total ice volume (a) and rate of ice loss (expressed as ice volume contributing to sea level rise per century) (b) through the deglaciation (26–5 kaBP) for the North American ice sheet (NAIS). Dark blue depicts the simulated NAIS using the GRISLI-iLOVECLIM set-up while the light blue envelop depicts the spread within the GRISLI stand-alone experiments (Methods). The ice sheet volume and rate of volume change of GLAC-1D (Tarasov et al., 2012) and ICE-6G (Peltier et al., 2015; Stuhne & Peltier, 2017) are shown in orange and red, respectively. The Bølling-Allerød warm period and the Younger Dryas cold period are shown by the pink vertical shading. The two melt-water pulses (MWPs) discussed in the text are in brown and the presence of the Lake Agassiz is shown by the horizontal green bar.

et al. (2018). We select the ensemble member that has the lowest root mean square error with respect to the present-day observed Antarctic ice sheet and we assume that the model parameters yielded for Antarctica are valid for the Northern Hemisphere ice sheets. However, we also use the local sediment thickness to facilitate sliding over areas displaying a thick sediment layer.

The climatic forcing that drives the ice sheet evolution is computed in two completely independent ways. In a first series of experiments the iLOVECLIM climate model (Roche, Dumas, et al., 2014; Roche, Paillard, et al., 2014) is bi-directionally coupled to GRISLI using a new downscaling capability (Quiquet, Roche, et al., 2018) to compute ice sheet surface mass balance from downscaled physical variables at the resolution of the ice sheet model for each atmospheric model time step. Surface mass balance is computed with an insolation - melt model (van den Berg et al., 2008) with local melt parameter tuning to partially correct for the model biases (Heinemann et al., 2014). Sub-shelf melting rate is computed from temperature and salinity provided by the ocean model (Beckmann & Goosse, 2003) and extrapolated to the ice sheet model grid, independently from marine- or lake-terminating margins. We use an acceleration of 10 for the forcings (greenhouse gas mixing ratio and orbital configuration) in order to reduce the time required to perform the experiments. The acceleration prevents us from considering the freshwater flux to the ocean resulting from ice sheet melting. The second series of experiments consist of a suite of ice sheet stand-alone experiments forced by an ensemble of synthetic climate histories that are elaborated from general circulation model (GCM) outputs and a proxy for temperature variability deduced from a Greenland ice core record (Charbit et al., 2007). In this case, the GCM last glacial maximum anomalies with respect to the pre-industrial from the PMIP3 database (Abe-Ouchi et al., 2015) are added to reanalysis data (Dee et al., 2011). Surface mass balance is here computed with a positive degree day model (Reeh, 1991). Climate changes at the southern margin of the NAIS and over Greenland were probably not synchronous and probably did not exhibit the same amplitude (e.g., Ivanovic et al., 2017). As such, these stand-alone experiments use an idealized climate forcing over the NAIS and they also may lack consistency between ice sheet and climate changes. They nonetheless provide an ensemble of alternative ice sheet evolutions during the deglaciation. More details on the modeling setup is given in the supporting information S1.

3. Results

Both sets of experiments produce deglacial NAIS volume losses in general agreement with the geologically constrained reconstructions (Figure 1a). However, in detail they do present some important differences. On the one hand, the stand-alone experiments show a pronounced millenial scale variability in ice volume, which is a direct consequence of the imposed atmospheric variability recorded in Greenland ice cores. In particular, the simulated NAIS loses ice up to a rate of 5 mSLE (meters of sea level equivalent) per century (Figure 1b) in response to the abrupt Bølling warming at 14.6 kaBP. That rate is comparable to the magnitude of the MWP-1A recorded in sea-level archives (Deschamps et al., 2012). These experiments show a second maximum in rate of volume loss toward the end of the Younger Dryas circa 11.5 kaBP, in agreement with the GLAC-1D reconstruction (Tarasov et al., 2012). On the other hand, in the coupled experiment, the gradual change in forcings (orbital and greenhouse gases) leads to a smoother simulated ice volume reduction. While ice volume between 26 and 17 kaBP is relatively stable, after this date, the ice loss rates are overestimated with respect to the geomorphological reconstructions, leading to a smaller simulated ice sheet extent (Figure S1 and S2). This faster ice sheet volume reduction in the coupled experiment is in part due to the fact that we do not account for the impact of meltwater flux to the ocean which are expected

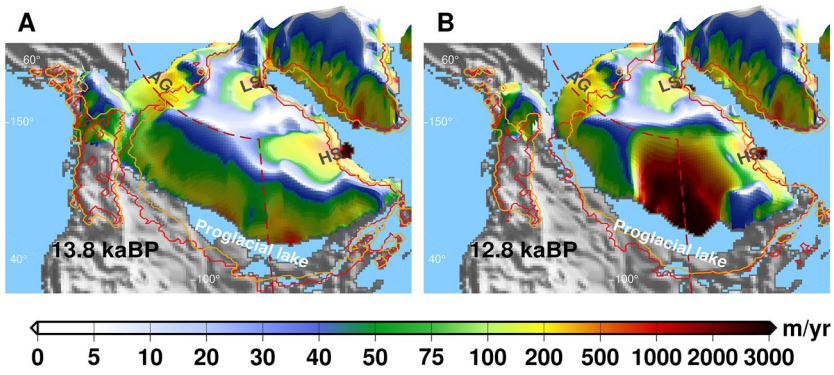

Figure 2. Ice sheet geometry at the time of the instability. Vertically integrated velocity in the coupled experiment for two snapshots, before (a) and after (b) the maximum in rate of ice loss for the North American ice sheet (NAIS). The two snapshots are separated by one thousand years. For this 3-D perspective plot, the velocity is draped on top of the ice sheet topography. The dashed line depicts the cross-section discussed in the main text. The major simulated ice streams are the Amundsen Gulf (AG), Lancaster Sound (LS) and Hudson Strait (HS) ice streams.

to weaken the North Atlantic overturning circulation and, as a result, to delay the Northern Hemisphere warming. Since the coupled model does not internally produce the Bølling warming, contrary to the stand-alone experiments in which such warming is imposed, it presents only one peak in rates of volume loss circa 13 kaBP of about 2 mSLE per century. It is interesting to notice that for the smallest value of the millenial scale variability in the stand-alone experiments, the volume loss rates show similarities with the coupled experiment since it shows only one maximum toward the end of the deglaciation (circa 10 kaBP using MPI-ESM-P, Figure S12 and supporting information S6). In the following, we show that the latest acceleration in ice loss, for the coupled and the stand-alone experiments, is due to the large proglacial lake that forms at the southern edge of the NAIS.

The pattern of our modeled NAIS retreat in the coupled experiment is illustrated in Figure 2 with two selected snapshots; one before and one after the timing of maximum rate of ice loss for the coupled experiment. The simulated ice sheet reproduces the major ice streams inferred by geomorphological observations (Hudson Strait, Lancaster Sound, Amundsen Gulf (Margold et al., 2018) on Figure 2). These ice streams are predominantly controlled by bedrock features (valleys, Figure S3) and terminate in the Atlantic and Arctic oceans. On the contrary, the continental southern margin does not show any well-identified ice stream. However, retreat of the ice sheet on its southern margin produced a large proglacial lake. This lake is a direct consequence of glacial isostasy since the glacial ice load in the model produced a largely depressed basin below the ice sheet. This simulated lake shows similarities with the proglacial lake Agassiz-Ojibway (Teller, 2003) for which we have evidence from about 13.4 kaBP before its drainage at 8.4 kaBP (Teller & Leverington, 2004). However, 13.8 kaBP is too early in the deglaciation to have a large lake as in Figure 2a. This mismatch in terms of timing is a direct consequence of the bias in the coupled experiment that presents a deglaciation that is too rapid (Figure S2). The stand-alone ice sheet experiments provide alternative ice sheet chronologies since various climate forcings can be used. While some of them also deglaciate too fast, others display a good agreement with ice sheet extent reconstructions (Figure S4).

The two selected snapshots of the coupled experiment (13.8 kaBP in Figures 2a and 12.8 kaB in Figure 2b) show a dramatic acceleration of the southern part of the ice sheet, associated with substantial grounding line retreat. Velocities of grounded ice shift from below 500 m yr^{-1} to about 2,000 m yr^{-1} in the vicinity of the grounding line. In the stand-alone experiments this rapid acceleration in ice sheet velocity is systematically reproduced independently from the climatic forcing, but it occurs later, from 12.2 to 9.6 kaBP (Figure S5). The timing of such event is weakly constrained as it is strongly linked with the deglacial geometry evolution. However, it is a robust feature of the deglaciation as it systematically occurs.

In Figure 3 we show a cross-section of the NAIS for the same temporal snapshots of Figure 2. At that time, the bedrock under the ice sheet is depressed with respect to its present-day value due to the glacial ice load

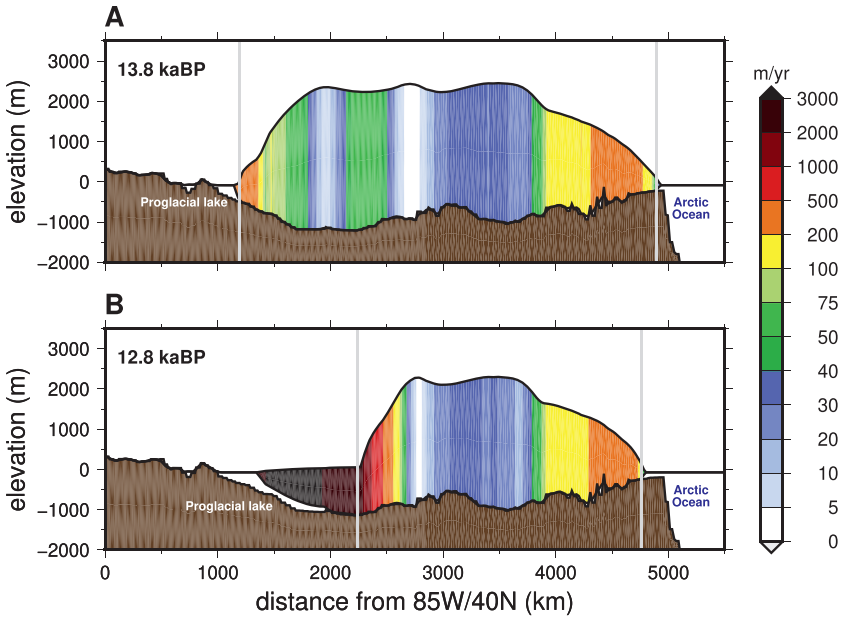

Figure 3. Bedrock profile. Cross-section of the North American ice sheet (NAIS) (dashed line on Figure 2) in the coupled experiment for two snapshots, before (a) and after (b) the maximum in rate of ice loss. The bedrock is depicted in brown color, the horizontal black line represents the contemporaneous eustatic sea level and the vertically averaged velocity is shown with the color palette. The vertical gray lines represent the position of the grounding line.

(Figure 3a). The southern margin of the ice sheet is thus resting on a reverse gradient bedrock slope. In the course of the deglaciation, the progressive thinning due to surface mass balance decrease leads eventually to floating terminus in the proglacial lake that formed at the southern ice sheet margin. Within one thousand years, the grounding line retreats by more than 700 km in the region of the simulated lake (Figure 3b). If surface mass balance explains most of the ice thickness change before 13.8 kaBP in the coupled experiment, the dynamical contribution becomes largely predominant once the instability is triggered (Figure S6). The ice sheet retreat switches to be mostly mechanically driven (supporting information S3). Interestingly, while another lake is simulated at the south-western margin of the NAIS (Figure 2), no rapid ice sheet destabilization is triggered there. This is due to the gentle bedrock slope there which only a produces a small grounding ice flux (Figure S7) and a more gradual retreat.

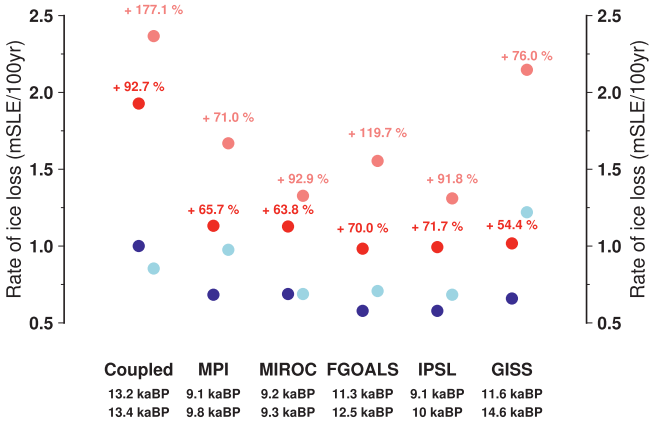

Figure 4. Importance of the lake level for the ice loss. Rate of ice loss toward the maximum of the continental grounding line instability event (red dots) and their contemporaneous values when we discard the impact of the proglacial lake on ice dynamics (blue dots) for the coupled model and different stand-alone experiments forced by PMIP3 models (Methods). The percentages indicate the loss rate increase induced by the proglacial lake. Light red dots represent the experiments in which we assume a lake level higher than the eustatic sea level (prescribed at +50 m above present-day sea level). Since the timing of the maximum in rate of ice loss differs for the different lake levels (earlier for higher lake level, indicated below the experiment label), the light blue dots (proglacial lake impact discarded) are not synchronous with the reference blue dots. The stand-alone experiments here use a weighing factor for the fast variability of 0.25.

To assess the importance of this lake-induced grounding line instability in shaping the deglaciation, we prevent its occurrence in a set of sensitivity experiments. To do so, we assume that the southern margin of the NAIS is perpetually grounded until 8 kaBP. Excluding the lake impact on ice floatation results in maximal rates of ice loss halved with respect to the experiments in which its effect is accounted for (Figure 4 and Figure S9). In particular, magnitude of local ice fluxes are an order of magnitude lower in the area of present-day Hudson Bay (Figure S10). The grounding line instability induced by the proglacial lake is thus a crucial process for the NAIS dynamics and explains the late deglacial acceleration of the ice sheet volume loss.

Since the lake induces a grounding line instability, the lake water depth plays a crucial role as it directly defines the floatation criteria. Our ice sheet model does not simulate explicitly proglacial lakes and

the lake surface elevation is assumed to follow the eustatic sea level. This is a conservative estimate since at high latitudes the water inputs to the lake exceed the evaporation and the water level is thus controlled by the elevation of the outlet. It is believed that large proglacial lakes at the southern margin of the NAIS presented probably a surface level about 100 m or more above the contemporaneous eustatic sea level (Clarke et al., 2004; Lambeck et al., 2017). For this reason, we performed additional experiments for which we assume a constant lake surface elevation at +50 m above present-day sea level in the NAIS southern margin area (about +120 m above eustatic sea level at 13 kaBP). In this case, the grounding line instability is enhanced and it often doubles the maximum ice loss rate compared to the simulations where the mechanism is inhibited (Figure 4 and Figure S10). While these additional experiments with a higher lake surface elevation lead to substantial difference in ice loss rates, we made additional computations that suggest that the elevation could be higher than +150 m above present-day sea-level in the course of the deglaciation (supporting information S4). This implies that if more realistic varying lake surface elevations were considered in our experiments, the grounding line instability induced by the lake would have been reinforced. As such, the implementation of an interactive depression-filling algorithm to infer the lake-water depth (e.g., Berends & van de Wal, 2016; Hinck, Gowan, & Lohmann, 2020) could be important to implement in ice sheet models to simulate the last deglaciation.

4. Discussion

The grounded line instability induced by the proglacial lake discussed in this study presents similarities with the MISI even though it also shows important differences. In the following we will refer to this instability as the proglacial lake ice sheet instability (PLISI). The first fundamental difference of the PLISI with respect to the MISI is that it occurs in a freshwater body. Present-day freshwater glaciers show calving and basal melting rates smaller than their tidewater analogs (Benn et al., 2007; Trüssel et al., 2013). It is thus possible that, in the proglacial lakes that existed at the ice sheet margin, such as Agassiz-Ojibway, the sub-shelf melt rate was small, or even that a certain amount of freezing of lake-water could occur below the ice shelves. In our experiments we do not apply any correcting factor to account for such differences with respect to salty waters. However, we perform a series of sensitivity experiments with varying sub-shelf melting and calving rates (supporting information S5 and Figure S11). We show that the PLISI is weakly sensitive to calving and sub-shelf melting rates because of the strongly negative surface mass balance at the southern margin of the NAIS during the deglaciation, however this might not always be the case for other time periods and/or ice sheets. Related to this, the predominance of surface mass balance with respect to the sub-shelf melt is another important difference with the MISI affecting the Antarctic ice sheet, where the oceanic forcing is there the main driver for grounding line instabilities.

The southern part of the NAIS has long been thought to retreat due to surface mass balance decrease in the course of the deglaciation. Here we have confirmed the conceptual idea first postulated by (Pollard, 1982) and advanced by (Fowler et al., 2013), and show that the PLISI provides an additional mechanism to facilitate the ice sheet retreat. In our simulations, the PLISI results in an acceleration of the deglaciation of the NAIS in its final stage, with rates of volume change of about 2 mSLE per century. The timing of the event is strongly linked to the chronology of the deglacial ice sheet geometries since it is a direct consequence of the floatation criteria, that is the local ice thickness. To avoid biasing the ice sheet response, we did not impose any external constraints on these geometries which can sometimes display substantial differences with geologically constrained reconstructions. Thus, we simulate a PLISI that happens as early as 13.8 kaBP for the coupled experiment that deglaciates too fast and between 12.2 and 9.6 kaBP for the standalone experiments. If these timings are very different they nonetheless represent a time when the simulated NAIS is largely retreated in its southern margin, reaching the region of the present-day Hudson Bay. In the reconstructed ice sheet extent data, this corresponds to about 11.5–9 kaBP where fan-like ice streams start emerging in the geological record (Margold et al., 2018). This coincides with the MWP-1B recorded at Barbados (Abdul et al., 2016) that could have occurred between 11.45 and 11.1 kaBP. The PLISI could have contributed to this event even though it should be confirmed with numerical experiments that show a better agreement with the geological record.

5. Conclusion and Perspectives

With a set of model simulations, we have shown that proglacial lakes can greatly influence ice sheet dynamics by providing a rapid grounding line retreat. The magnitude and the timing of this rapid grounding line retreat likely depends on the evolution of the ice sheet geometry, however, the instability systematically occurs during the course of the deglaciation as a result of glacioisostatic depression. Differing from the MISI, the grounding line instability discussed in this study is only weakly sensitive to calving and lake subshelf melting rates because of the strongly negative surface mass balance at the NAIS southern margin. The lake induces an ice sheet retreat that is almost entirely mechanically driven although initially triggered by a decrease in surface mass balance. As such, it is a self-sustained instability that can maintain large ice sheet volume loss regardless of later climate change. In our simulations, the PLISI induces maximum rates of volume change of about 2 mSLE per century.

This mechanism raises a number of scientific questions as we have no contemporaneous analogs, although a large number of outlet glaciers, notably in Patagonia, Greenland and Antarctica, terminate in proglacial lakes (Carrivick & Tweed, 2013). These glaciers do not allow for large floating ice shelves. Instead, at the ice sheet scale, the PLISI could have generated large and thick ice shelves floating over freshwater cavities.

If the PLISI mechanism is crucial to understand the deglaciation of the NAIS, it will be as important for the Eurasian ice sheet. Large proglacial lakes were also present at the southern flank of the Eurasian ice sheet, in the vicinity of the Baltic and White seas (Patton et al., 2017). The PLISI could be a mechanism that explains the observed cyclicity in abrupt discharge events recorded in the Black sea (Soulet et al., 2013). More generally, the PLISI could be crucial to understand deglacial Pleistocene eustatic sea level.

This highlights the need for a better representation of the proglacial lakes in continental ice sheet models, which is becoming an active field of research in the community. At the glacier scale, fine-scale interactions are now becoming explicitly represented in numerical models (Carrivick et al., 2020) and the effect of lakes on valley glacier retreat has been quantified (Sutherland et al., 2020). At the ice sheet scale, algorithms to compute interactively the lake-water depth for a changing ice sheet geometry are becoming more common (Berends & van de Wal, 2016; Hinck, Gowan, & Lohmann, 2020) and bi-directional coupled lake model and ice sheet model have recently emerged (Hinck, Gowan, Zhang, & Lohmann, 2020).

While grounding line dynamics is a well-established process to account for the Antarctic ice sheet evolution, the PLISI mechanism is another manifestation of its importance to trigger large acceleration of continental ice sheet retreat. These results highlight the need for a good understanding of grounding line physics and its representation in numerical models in order to reduce the uncertainties on sea level projections for the ongoing deglaciation.

Data Availability Statement

Source data of the figures presented in the main text of the manuscript are available on the Zenodo repository with digital object identifier 10.5281/zenodo.4629216 (Quiquet et al., 2021).

Acknowledgments
The research leading to these results has received funding from the European Research Council under the European Union's Seventh Framework Program (FP7/2007-2013 Grant agreement n° 339108) and from the SCOR foundation project COASTRISK.

References

Abdul, N. A., Mortlock, R. A., Wright, J. D., & Fairbanks, R. G. (2016). Younger Dryas sea level and meltwater pulse 1B recorded in Barbados reef crest coral Acropora palmata. *Paleoceanography*, *31*(2), 330–344. https://doi.org/10.1002/2015PA002847

Abe-Ouchi, A., Saito, F., Kageyama, M., Braconnot, P., Harrison, S. P., Lambeck, K., et al. (2015). Ice-sheet configuration in the CMIP5/PMIP3 last glacial maximum experiments. *Geoscientific Model Development*, *8*(11), 3621–3637. https://doi.org/10.5194/gmd-8-3621-2015

Abe-Ouchi, A., Saito, F., Kawamura, K., Raymo, M. E., Okuno, J, Takahashi, K., & Blatter, H. (2013). Insolation-driven 100,000-year glacial cycles and hysteresis of ice-sheet volume. *Nature*, *500*(7461), 190–193. https://doi.org/10.1038/nature12374

Barber, D. C., Dyke, A., Hillaire-Marcel, C., Jennings, A. E., Andrews, J. T., Kerwin, M. W., et al. (1999). Forcing of the cold event of 8,200 years ago by catastrophic drainage of Laurentide lakes. *Nature*, *400*(6742), 344–348. https://doi.org/10.1038/22504

Beckmann, A., & Goosse, H. (2003). A parameterization of ice shelf-ocean interaction for climate models. *Ocean Modelling*, *5*(2), 157–170. https://doi.org/10.1016/S1463-5003(02)00019-7

Benn, D. I., Warren, C. R., & Mottram, R. H. (2007). Calving processes and the dynamics of calving glaciers. *Earth-Science Reviews*, *82*(3), 143–179. https://doi.org/10.1016/j.earscirev.2007.02.002

Berends, C. J., & van de Wal, R. S. W. (2016). A computationally efficient depression-filling algorithm for digital elevation models, applied to proglacial lake drainage. *Geoscientific Model Development*, *9*(12), 4451–4460. https://doi.org/10.5194/gmd-9-4451-2016

Calov, R., Ganopolski, A., Petoukhov, V., Claussen, M., & Greve, R. (2002). Large-scale instabilities of the Laurentide ice sheet simulated in a fully coupled climate-system model. *Geophysical Research Letters*, *29*(24), 69-1-69-4. https://doi.org/10.1029/2002GL016078

Carrivick, J. L., & Tweed, F. S. (2013). Proglacial lakes: Character, behaviour and geological importance. *Quaternary Science Reviews*, *78*, 34–52. https://doi.org/10.1016/j.quascirev.2013.07.028

Carrivick, J. L., Tweed, F. S., Sutherland, J. L., & Mallalieu, J. (2020). Toward numerical modeling of interactions between ice-marginal proglacial lakes and glaciers. *Frontiers of Earth Science*, *8*, 500. https://doi.org/10.3389/feart.2020.577068

Charbit, S., Kageyama, M., Roche, D., Ritz, C., & Ramstein, G. (2005). Investigating the mechanisms leading to the deglaciation of past continental northern hemisphere ice sheets with the CLIMBER-GREMLINS coupled model. *Global and Planetary Change*, *48*, 253–273. https://doi.org/10.1016/j.gloplacha.2005.01.002

Charbit, S., Ritz, C., Philippon, G., Peyaud, V., & Kageyama, M. (2007). Numerical reconstructions of the Northern Hemisphere ice sheets through the last glacial-interglacial cycle. *Climate of the Past*, *3*, 15–37. https://doi.org/10.5194/cp-3-15-2007

Clarke, G. K. C., Leverington, D. W., Teller, J. T., & Dyke, A. S. (2004). Paleohydraulics of the last outburst flood from glacial Lake Agassiz and the 8200BP cold event. *Quaternary Science Reviews*, *23*(3), 389–407. https://doi.org/10.1016/j.quascirev.2003.06.004

DeConto, R. M., & Pollard, D. (2016). Contribution of Antarctica to past and future sea-level rise. *Nature*, *531*(7596), 591–597. https://doi.org/10.1038/nature17145

Dee, D. P., Uppala, S. M., Simmons, A. J., Berrisford, P., Poli, P., Kobayashi, S., et al. (2011). The ERA-Interim reanalysis: Configuration and performance of the data assimilation system. *Quarterly Journal of the Royal Meteorological Society*, *137*(656), 553–597. https://doi.org/10.1002/qj.828

Deschamps, P., Durand, N., Bard, E., Hamelin, B., Camoin, G., Thomas, A. L., et al. (2012). Ice-sheet collapse and sea-level rise at the Bølling warming 14,600 years ago. *Nature*, *483*(7391), 559–564. https://doi.org/10.1038/nature10902

Favier, L., Durand, G., Cornford, S. L., Gudmundsson, G. H., Gagliardini, O., Gillet-Chaulet, F., et al. (2014). Retreat of Pine Island Glacier controlled by marine ice-sheet instability. *Nature Climate Change*, *4*(2), 117–121. https://doi.org/10.1038/nclimate2094

Fowler, A. C., Rickaby, R. E. M., & Wolff, E. W. (2013). Exploration of a simple model for ice ages. *International Journal of Geometry*, *4*(2), 227–297. https://doi.org/10.1007/s13137-012-0040-7

Ganopolski, A., & Brovkin, V. (2017). Simulation of climate, ice sheets and CO2 evolution during the last four glacial cycles with an Earth system model of intermediate complexity. *Climate of the Past*, *13*(12), 1695–1716. https://doi.org/10.5194/cp-13-1695-2017

Goelzer, H., Nowicki, S., Payne, A., Larour, E., Seroussi, H., Lipscomb, W. H, et al. (2020). The future sea-level contribution of the Greenland ice sheet: A multi-model ensemble study of ISMIP6. *The Cryosphere*, *14*(9), 3071–3096. https://doi.org/10.5194/tc-14-1747-2020

Gregoire, L. J., Otto-Bliesner, B., Valdes, P. J., & Ivanovic, R. (2016). Abrupt Bølling warming and ice saddle collapse contributions to the Meltwater Pulse 1a rapid sea level rise. *Geophysical Research Letters*, *43*(17), 9130–9137. https://doi.org/10.1002/2016GL070356

Gregoire, L. J., Payne, A. J., & Valdes, P. J. (2012). Deglacial rapid sea level rises caused by ice-sheet saddle collapses. *Nature*, *487*(7406), 219–222. https://doi.org/10.1038/nature11257

Heinemann, M., Timmermann, A., Elison Timm, O., Saito, F., & Abe-Ouchi, A. (2014). Deglacial ice sheet meltdown: Orbital pacemaking and CO2 effects. *Climate of the Past*, *10*(4), 1567–1579. https://doi.org/10.5194/cp-10-1567-2014

Hinck, S., Gowan, E. J., & Lohmann, G. (2020). LakeCC: A tool for efficiently identifying lake basins with application to palaeogeographic reconstructions of North America. *Journal of Quaternary Science*, *35*(3), 422–432. https://doi.org/10.1002/jqs.3182

Hinck, S., Gowan, E. J., Zhang, X., & Lohmann, G. (2020). PISM-LakeCC: Implementing an adaptive proglacial lake boundary into an ice sheet model. *The Cryosphere Discussions*, 1–36. https://doi.org/10.5194/tc-2020-353

Hostetler, S. W., Bartlein, P. J., Clark, P. U., Small, E. E., & Solomon, A. M. (2000). Simulated influences of Lake Agassiz on the climate of central North America 11,000 years ago. *Nature*, *405*(6784), 334–337. https://doi.org/10.1038/35012581

Ivanovic, R. F., Gregoire, L. J., Wickert, A. D., Valdes, P. J., & Burke, A. (2017). Collapse of the North American ice saddle 14,500 years ago caused widespread cooling and reduced ocean overturning circulation. *Geophysical Research Letters*, *44*, 383–392. https://doi.org/10.1002/2016GL071849

Krinner, G., Mangerud, J., Jakobsson, M., Crucifix, M., Ritz, C., & Svendsen, J. I. (2004). Enhanced ice sheet growth in Eurasia owing to adjacent ice-dammed lakes. *Nature*, *427*(6973), 429–432. https://doi.org/10.1038/nature02233

Lambeck, K., Purcell, A., & Zhao, S. (2017). The North American Late Wisconsin ice sheet and mantle viscosity from glacial rebound analyses. *Quaternary Science Reviews*, *158*, 172–210. https://doi.org/10.1016/j.quascirev.2016.11.033

Lambeck, K., Rouby, H., Purcell, A., Sun, Y., & Sambridge, M. (2014). Sea level and global ice volumes from the Last Glacial Maximum to the Holocene. *Proceedings of the National Academy of Sciences*, *111*(43), 15296–15303. https://doi.org/10.1073/pnas.1411762111

Larour, E., Seroussi, H., Morlighem, M., & Rignot, E. (2012). Continental scale, high order, high spatial resolution, ice sheet modeling using the Ice Sheet System Model (ISSM). *Journal of Geophysical Research*, *117*, F01022. https://doi.org/10.1029/2011JF002140

Levermann, A., Winkelmann, R., Albrecht, T., Goelzer, H., Golledge, N. R., Greve, R., et al. (2020). Projecting Antarctica's contribution to future sea level rise from basal ice shelf melt using linear response functions of 16 ice sheet models (LARMIP-2). *Earth System Dynamics*, *11*(1), 35–76. https://doi.org/10.5194/esd-11-35-2020

MacAyeal, D. R. (1993). Binge/purge oscillations of the Laurentide Ice Sheet as a cause of the North Atlantic's Heinrich events. *Paleoceanography*, *8*(6), 775–784. https://doi.org/10.1029/93PA02200

Margold, M., Stokes, C. R., & Clark, C. D. (2018). Reconciling records of ice streaming and ice margin retreat to produce a palaeogeographic reconstruction of the deglaciation of the Laurentide Ice Sheet. *Quaternary Science Reviews*, *189*, 1–30. https://doi.org/10.1016/j.quascirev.2018.03.013

Patton, H., Hubbard, A., Andreassen, K., Auriac, A., Whitehouse, P. L., Stroeven, A. P., et al. (2017). Deglaciation of the Eurasian ice sheet complex. *Quaternary Science Reviews*, *169*, 148–172. https://doi.org/10.1016/j.quascirev.2017.05.019

Pattyn, F., Perichon, L., Durand, G., Favier, L., Gagliardini, O., Hindmarsh, R. C. A., et al. (2013). Grounding-line migration in plan-view marine ice-sheet models: Results of the ice2sea MISMIP3d intercomparison. *Journal of Glaciology*, *59*(215), 410–422. https://doi.org/10.3189/2013JoG12J129

Peltier, W. R., Argus, D. F., & Drummond, R. (2015). Space geodesy constrains ice age terminal deglaciation: The global ICE-6G_c (VM5a) model. *Journal of Geophysical Research: Solid Earth*, *120*(1), 450–487. https://doi.org/10.1002/2014JB011176

Pollard, D. (1982, March). A simple ice sheet model yields realistic 100 kyr glacial cycles. *Nature*, *296*(5855), 334–338. https://doi.org/10.1038/296334a0

Quiquet, A., & Dumas, C. (2021a). The GRISLI-LSCE contribution to the Ice Sheet Model Intercomparison Project for phase 6 of the Coupled Model Intercomparison Project (ISMIP6) - Part 1: Projections of the Greenland ice sheet evolution by the end of the 21st century. *The Cryosphere*, *15*(2), 1015–1030. https://doi.org/10.5194/tc-15-1015-2021

Quiquet, A., & Dumas, C. (2021b). The GRISLI-LSCE contribution to the Ice Sheet Model Intercomparison Project for phase 6 of the Coupled Model Intercomparison Project (ISMIP6) - Part 2: Projections of the Antarctic ice sheet evolution by the end of the 21st century. *The Cryosphere*, *15*(2), 1031–1052. https://doi.org/10.5194/tc-15-1031-2021

Quiquet, A., Dumas, C., Paillard, D., Ramstein, G., Ritz, C., & Roche, D. M. (2021). *Deglacial ice sheet instabilities induced by proglacial lakes*. Zenodo. (type: dataset). https://doi.org/10.5281/zenodo.4629216

Quiquet, A., Dumas, C., Ritz, C., Peyaud, V., & Roche, D. M. (2018). The GRISLI ice sheet model (version 2.0): Calibration and validation for multi-millennial changes of the Antarctic ice sheet. *Geoscientific Model Development*, *11*(12), 5003–5025. https://doi.org/10.5194/gmd-11-5003-2018

Quiquet, A., Roche, D. M., Dumas, C., & Paillard, D. (2018). Online dynamical downscaling of temperature and precipitation within the iLOVECLIM model (version 1.1). *Geoscientific Model Development*, *11*(1), 453–466. https://doi.org/10.5194/gmd-11-453-2018

Reeh, N. (1991). Parameterization of melt rate and surface temperature on the Greenland Ice Sheet. *Polarforschung*, *59*(3), 113–128.

Roche, D. M., Dumas, C., Bügelmayer, M., Charbit, S., & Ritz, C. (2014). Adding a dynamical cryosphere to iLOVECLIM (version 1.0): Coupling with the GRISLI ice-sheet model. *Geoscientific Model Development*, *7*(4), 1377–1394. https://doi.org/10.5194/gmd-7-1377-2014

Roche, D. M., Paillard, D., Caley, T., & Waelbroeck, C. (2014). LGM hosing approach to Heinrich Event 1: Results and perspectives from data-model integration using water isotopes. *Quaternary Science Reviews*, *106*, 247–261. https://doi.org/10.1016/j.quascirev.2014.07.020

Schoof, C. (2007). Ice sheet grounding line dynamics: Steady states, stability, and hysteresis. *Journal of Geophysical Research*, *112*, F03S28. https://doi.org/10.1029/2006jf000664

Seroussi, H., Nowicki, S., Payne, A. J., Goelzer, H., Lipscomb, W. H., Abe-Ouchi, A., et al. (2020). ISMIP6 Antarctica: A multi-model ensemble of the Antarctic ice sheet evolution over the 21st century. *The Cryosphere*, *14*(9), 3033–3070. https://doi.org/10.5194/tc-14-3033-2020

Soulet, G., Ménot, G., Bayon, G., Rostek, F., Ponzevera, E., Toucanne, S., et al. (2013). Abrupt drainage cycles of the Fennoscandian Ice Sheet. *Proceedings of the National Academy of Sciences*, *110*(17), 6682–6687. https://doi.org/10.1073/pnas.1214676110

Stuhne, G. R., & Peltier, W. R. (2017). Assimilating the ICE-6G_C reconstruction of the Latest Quaternary Ice Age Cycle into numerical simulations of the Laurentide and Fennoscandian Ice Sheets. *Journal of Geophysical Research: Earth Surface*, *122*, 2324–2347. https://doi.org/10.1002/2017JF004359

Sun, S., Pattyn, F., Simon, E. G., Albrecht, T., Cornford, S., Calov, R., et al. (2020). Antarctic ice sheet response to sudden and sustained ice-shelf collapse (ABUMIP). *Journal of Glaciology*, *66*, 891–904. https://doi.org/10.1017/jog.2020.67

Sutherland, J. L., Carrivick, J. L., Gandy, N., Shulmeister, J., Quincey, D. J., & Cornford, S. L. (2020). Proglacial Lakes Control Glacier Geometry and Behavior During Recession. *Geophysical Research Letters*, *47*, e2020GL088865. https://doi.org/10.1029/2020gl088865

Tarasov, L., Dyke, A. S., Neal, R. M., & Peltier, W. R. (2012). A data-calibrated distribution of deglacial chronologies for the North American ice complex from glaciological modeling. *Earth and Planetary Science Letters*, *315–316*, 30–40. https://doi.org/10.1016/j.epsl.2011.09.010

Teller, J. T. (1995). History and drainage of large ice-dammed lakes along the Laurentide Ice Sheet. *Quaternary International*, *28*, 83–92. https://doi.org/10.1016/1040-6182(95)00050-S

Teller, J. T. (2003). Controls, history, outbursts, and impact of large late-Quaternary proglacial lakes in North America. In.*Developments in quaternary sciences* (pp. 45–61). Elsevier. https://doi.org/10.1016/S1571-0866(03)01003-0

Teller, J. T., & Leverington, D. W. (2004). Glacial Lake Agassiz: A 5000 yr history of change and its relationship to the δ18O record of Greenland. *Geological Society of America Bulletin*, *116*(5–6), 729–742. https://doi.org/10.1130/B25316.1

Trüssel, B. L., Motyka, R. J., Truffer, M., & Larsen, C. F. (2013). Rapid thinning of lake-calving Yakutat Glacier and the collapse of the Yakutat Icefield, southeast Alaska, USA. *Journal of Glaciology*, *59*(213), 149–161. https://doi.org/10.3189/2013J0G12J081

Tsai, V. C., Stewart, A. L., & Thompson, A. F. (2015). Marine ice-sheet profiles and stability under Coulomb basal conditions. *Journal of Glaciology*, *61*(226), 205–215. https://doi.org/10.3189/2015JoG14J221

van den Berg, J., van de Wal, R., & Oerlemans, H. (2008). A mass balance model for the Eurasian Ice Sheet for the last 120,000 years. *Global and Planetary Change*, *61*(3), 194–208. https://doi.org/10.1016/j.gloplacha.2007.08.015

Weertman, J. (1974). Stability of the junction of an ice sheet and an ice shelf. *Journal of Glaciology*, *13*(67), 3–11. https://doi.org/10.3189/S0022143000023327

Wiersma, A. P., & Renssen, H. (2006,). Model-data comparison for the 8.2kaBP event: Confirmation of a forcing mechanism by catastrophic drainage of Laurentide Lakes. *Quaternary Science Reviews*, *25*(1), 63–88. https://doi.org/10.1016/j.quascirev.2005.07.009

Winkelmann, R., Martin, M. A., Haseloff, M., Albrecht, T., Bueler, E., Khroulev, C., & Levermann, A. (2011). The Potsdam Parallel Ice Sheet Model (PISM-PIK) - Part 1: Model description. *The Cryosphere*, *5*(3), 715–726. https://doi.org/10.5194/tc-5-715-2011